

## Supplementary Information

# The Cu-Al<sub>2</sub>O<sub>3</sub> Interface: An Unignorable Active Site for Methanol Steam Reforming Hydrogen Production

Qianlong Mao<sup>1</sup>, Xiaohui Liu<sup>1</sup>, Yong Guo<sup>1,\*</sup>, Yanqin Wang<sup>1</sup>

<sup>1</sup> State Key Laboratory of Green Chemical Engineering and Industrial Catalysis, School of Chemistry and Molecular Engineering, School of Chemistry and Molecular Engineering, East China University of Science and Technology, Shanghai 200237, P. R. China.

\*Corresponding Author: Yong Guo, [guoyong@ecust.edu.cn](mailto:guoyong@ecust.edu.cn)

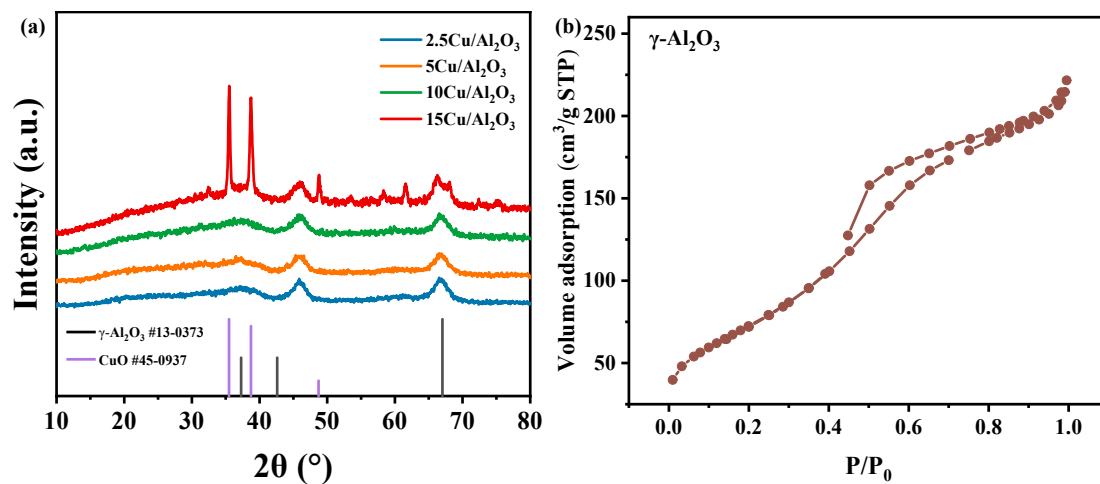


**Fig. S1.** (a) XRD patterns of the fresh catalysts. (b) Nitrogen physisorption isotherms of  $\gamma\text{-Al}_2\text{O}_3$ .

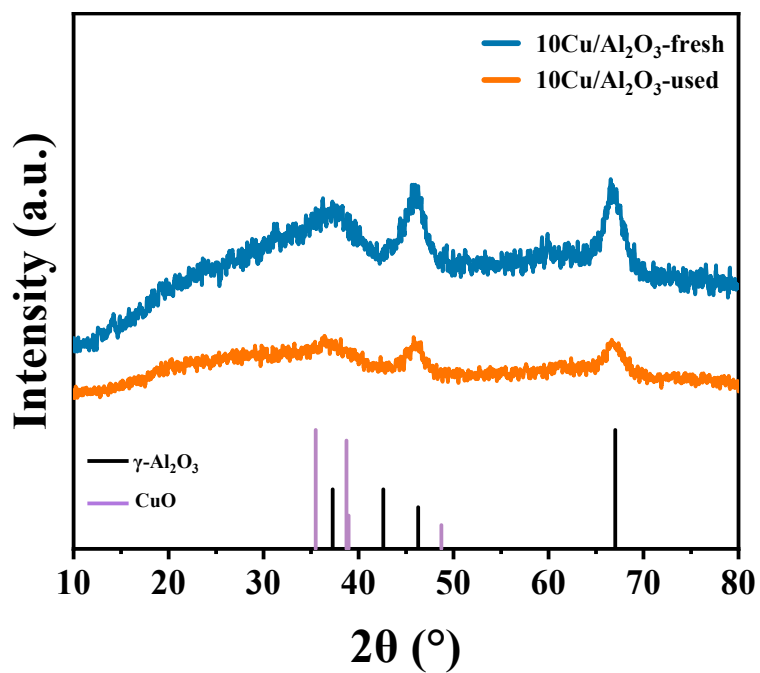


**Fig. S2.** XRD patterns of the fresh and used  $10\text{Cu}/\text{Al}_2\text{O}_3$  catalysts.

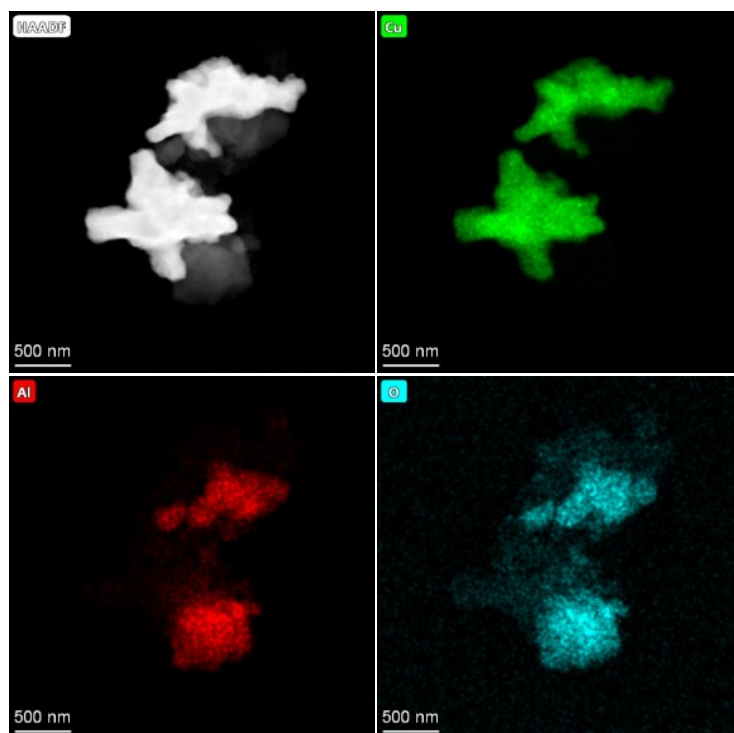


**Fig. S3.** High-angle annular dark-field STEM images of 15Cu/Al<sub>2</sub>O<sub>3</sub>, corresponding EDS elemental maps.

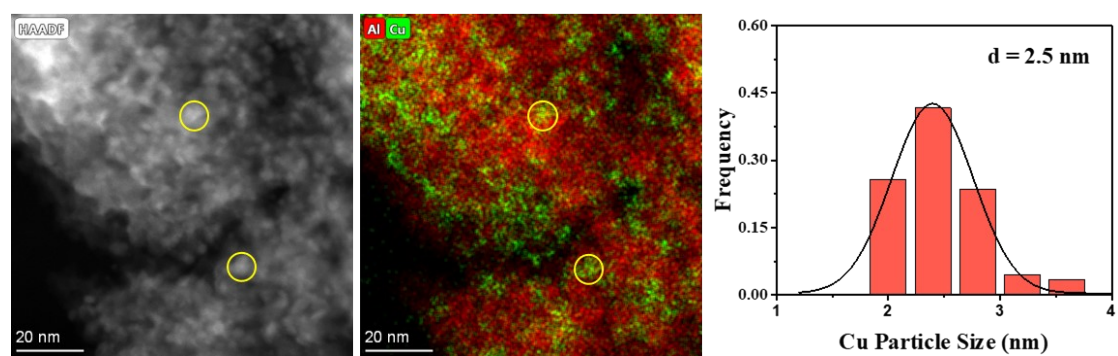


**Fig. S4.** High-angle annular dark-field STEM images of 10Cu/Al<sub>2</sub>O<sub>3</sub>-used, corresponding EDS elemental maps and size distribution.

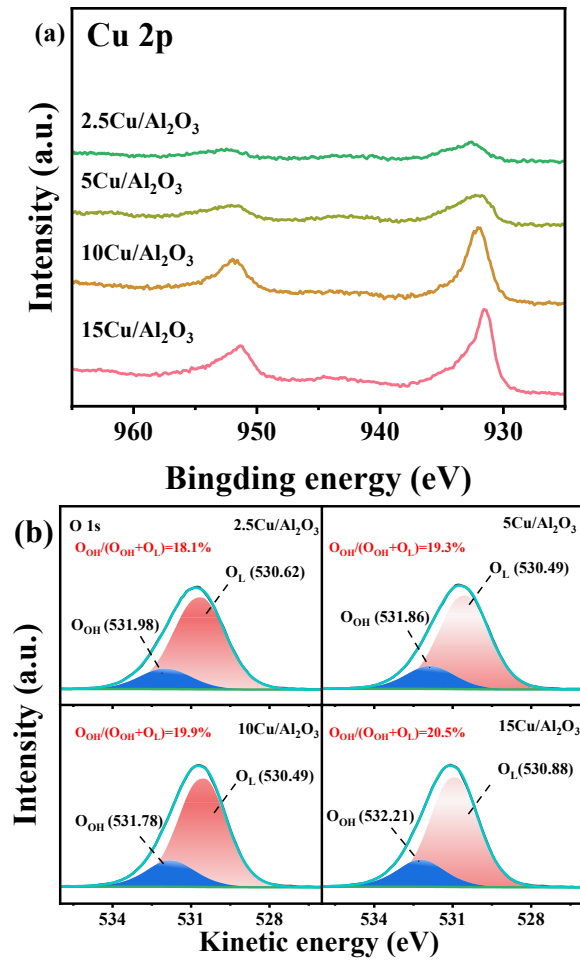


**Fig. S5.** Quasi *in-situ* X-ray photoelectron spectroscopy spectra of (a) Cu 2p and (b) O 1s.

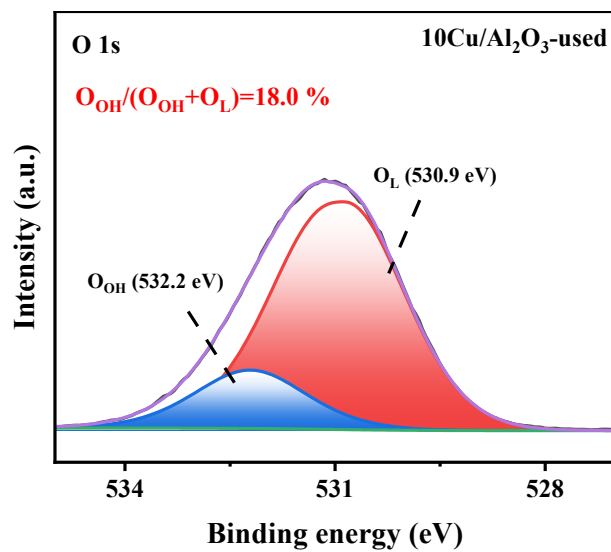


**Fig. S6.** Quasi *in-situ* O 1s XPS spectra of 10Cu/Al<sub>2</sub>O<sub>3</sub>-used.

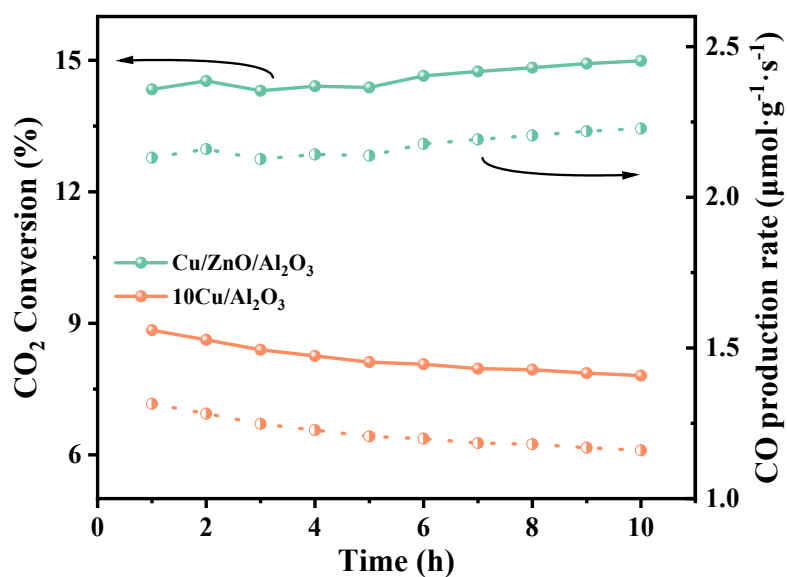


**Fig. S7.** Catalytic performance of 10Cu/Al<sub>2</sub>O<sub>3</sub> and commercial Cu/ZnO/Al<sub>2</sub>O<sub>3</sub> catalysts for reverse water-gas shift at 250 °C. Reaction conditions: 0.1 Mpa, gas flow rate 20 mL·min<sup>-1</sup> for 10%CO<sub>2</sub>/30%H<sub>2</sub>/60%N<sub>2</sub>, 0.1 g catalyst, WHSV = 12000 mL·g<sup>-1</sup>·h<sup>-1</sup>.

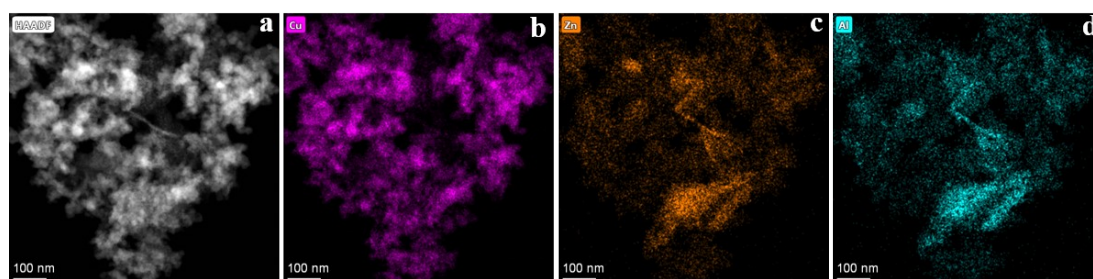


**Fig. S8.** (a) High-angle annular dark-field STEM images, corresponding (b, c, d) EDS elemental maps of reduced Cu/ZnO/Al<sub>2</sub>O<sub>3</sub>.

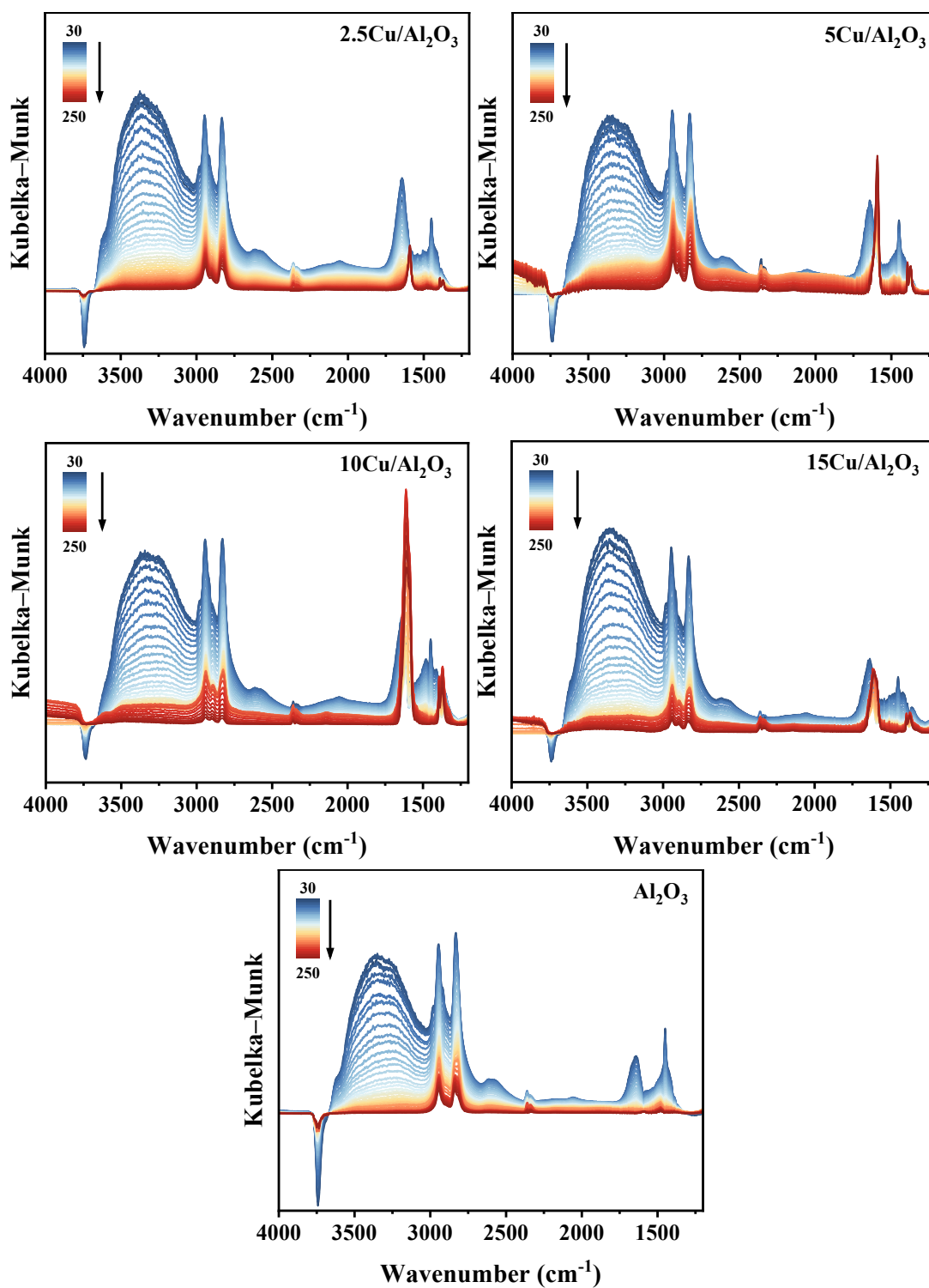


**Fig. S9.** *In-situ* temperature-programmed DRIFTS of  $m\text{Cu}/\text{Al}_2\text{O}_3$  with the spectra collected with an increasing temperature to 250 °C in Ar after preadsorption of methanol and water at 30 °C.

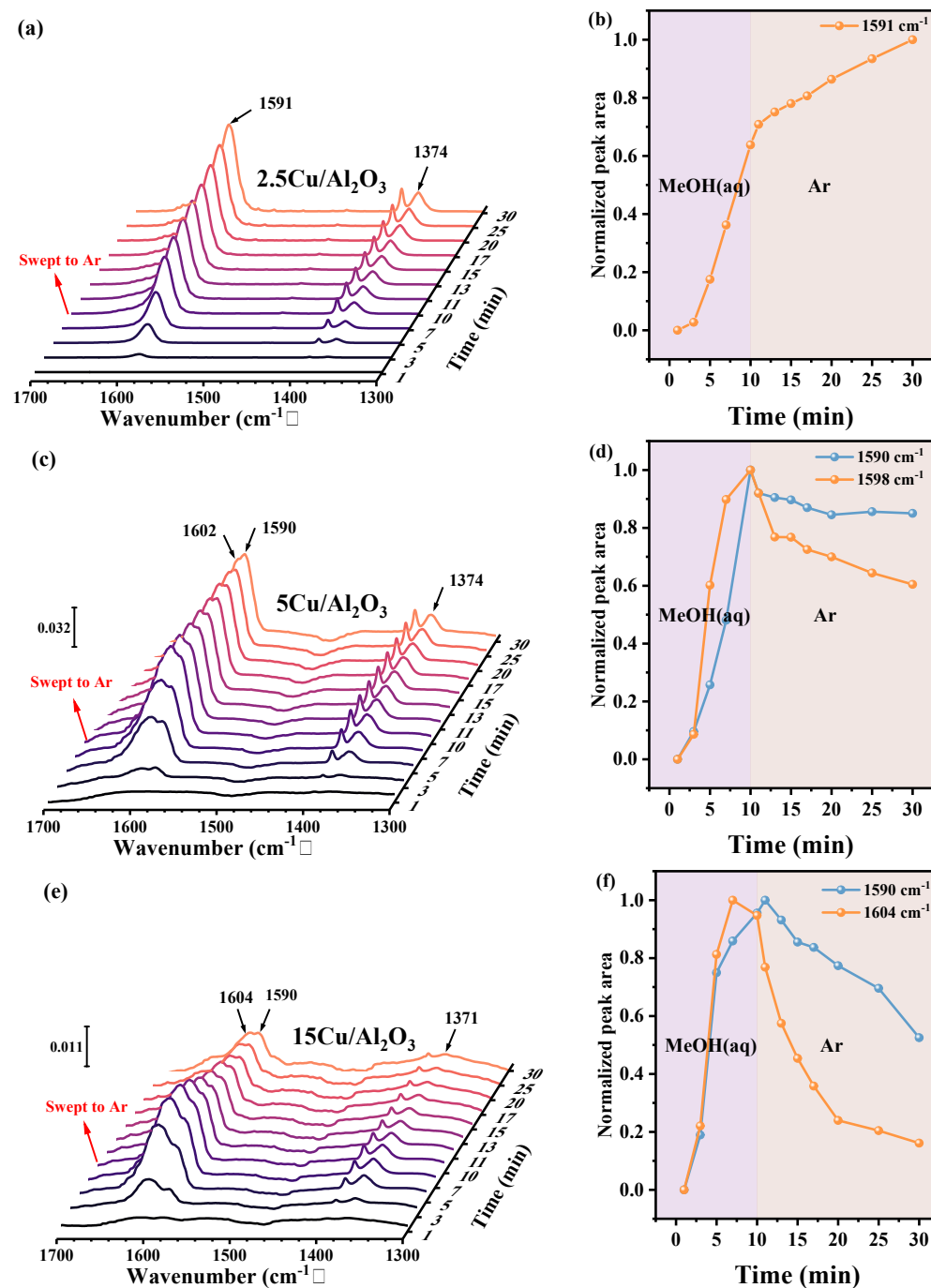


**Fig. S10.** *In-situ* DRIFTS of MSR on (a) 2.5Cu/Al<sub>2</sub>O<sub>3</sub>, (c) 5Cu/Al<sub>2</sub>O<sub>3</sub>, and (e) 15Cu/Al<sub>2</sub>O<sub>3</sub> exposed to the mixture of CH<sub>3</sub>OH/H<sub>2</sub>O for 10 min and followed Ar flushing for another 20 min at 250 °C; variations in the peak areas of two different surface formates (1590 cm<sup>-1</sup>) and (1602 cm<sup>-1</sup>) on (b) 2.5Cu/Al<sub>2</sub>O<sub>3</sub>, (d) 5Cu/Al<sub>2</sub>O<sub>3</sub>, and (f) 15Cu/Al<sub>2</sub>O<sub>3</sub>, respectively.

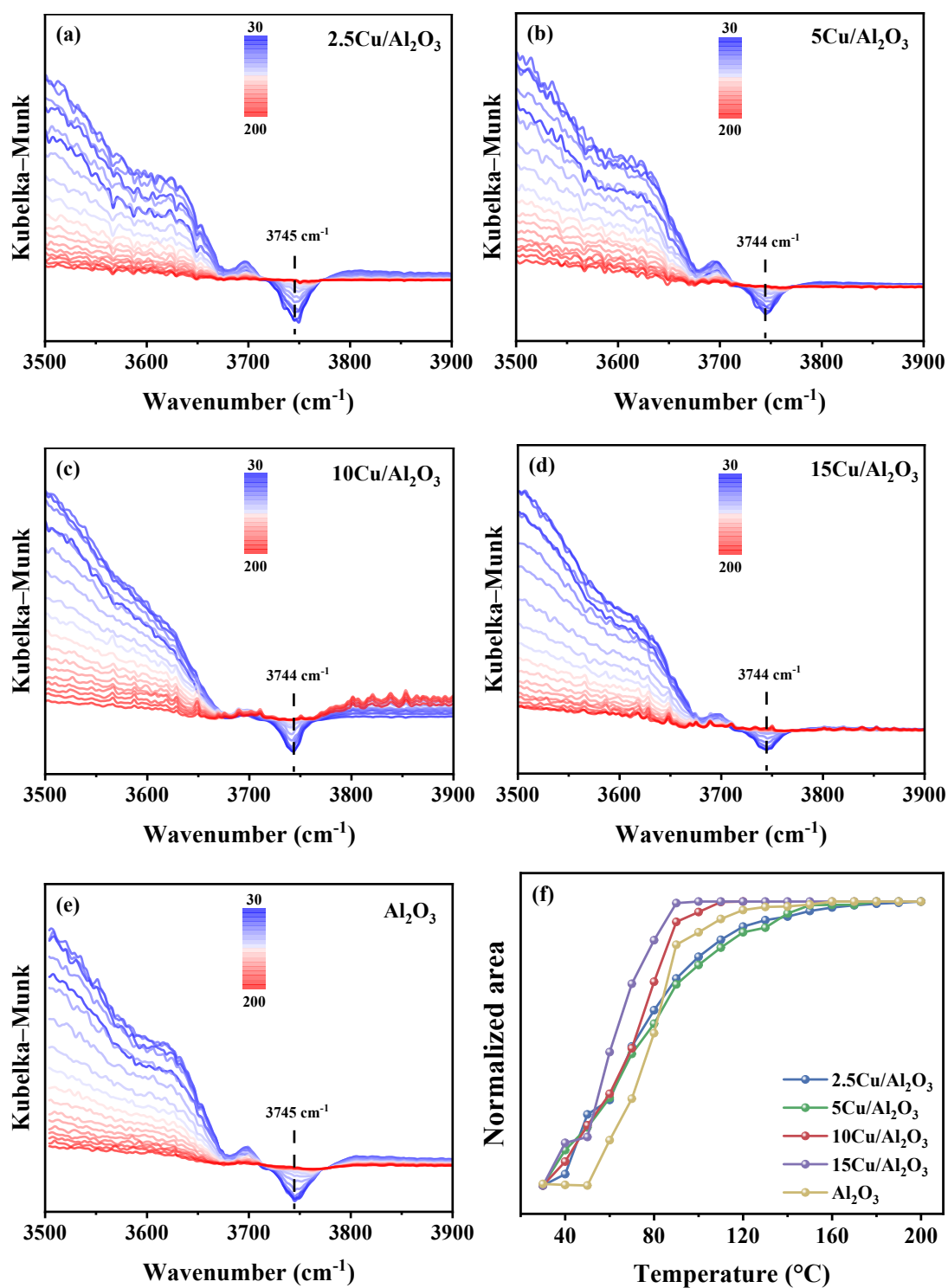


**Fig. S11.** (a-e) *In-situ* temperature-programmed DRIFTS of mCu/Al<sub>2</sub>O<sub>3</sub> with the spectra collected with an increasing temperature to 200 °C in Ar after preadsorption of water at 30 °C. (f) The integrated peak area of surface hydroxyl (3744 cm<sup>-1</sup>) versus temperature during temperature ramping.



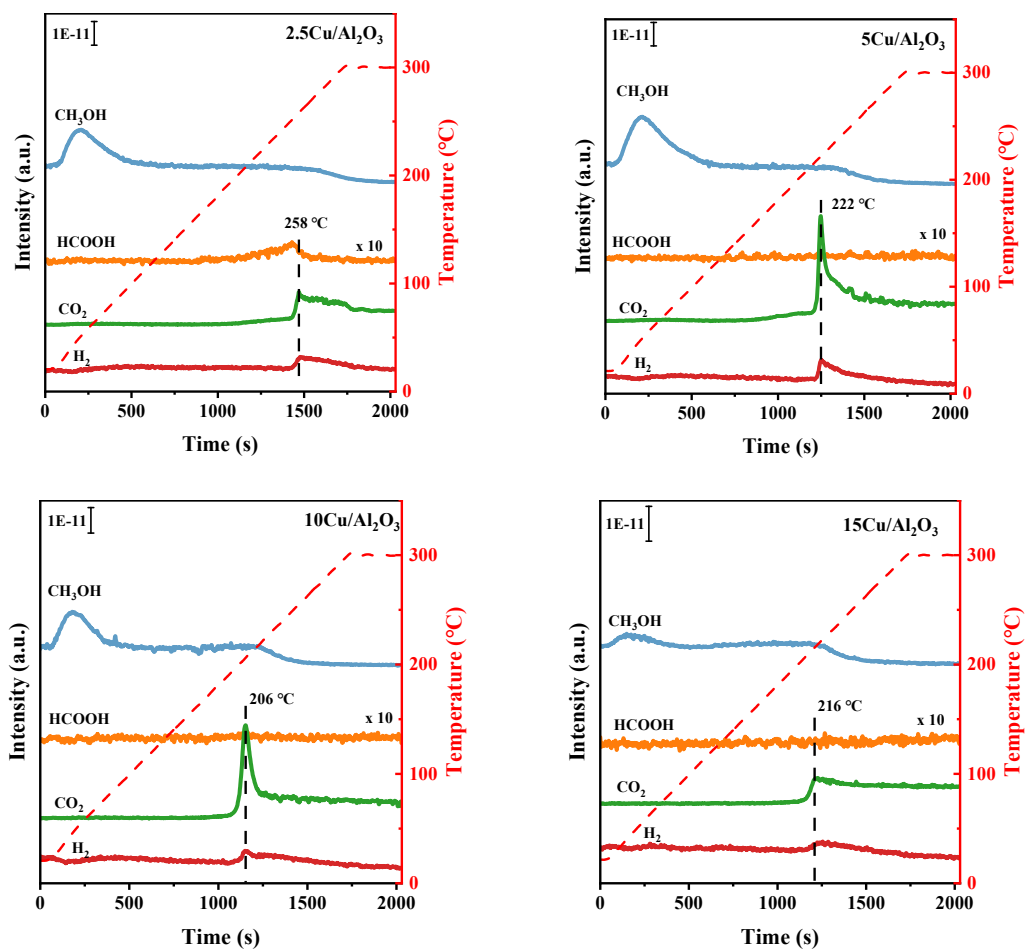


**Fig. S12.** Temperature-programmed surface reaction (TPSR) of MSR on mCu/Al<sub>2</sub>O<sub>3</sub> catalysts.

**Table S1.** Physicochemical properties of catalysts

Samples	BET (m <sup>2</sup> ·g <sup>-1</sup> ) <sup>a</sup>	Average pore diameter (nm) <sup>b</sup>	Content of Cu (%) <sup>c</sup>	D <sub>Cu</sub> (%) <sup>d</sup>	d <sub>Cu</sub> (nm) <sup>e</sup>
2.5Cu/Al <sub>2</sub> O <sub>3</sub>	239.3	4.6	2.5	95.8	1.6
5Cu/Al <sub>2</sub> O <sub>3</sub>	250.6	4.5	5.0	54.2	1.9
10Cu/Al <sub>2</sub> O <sub>3</sub>	227.2	4.7	9.2	26.9	2.1
15Cu/Al <sub>2</sub> O <sub>3</sub>	242.4	4.5	15.0	12.4	2.5
10Al <sub>2</sub> O <sub>3</sub> /Cu	37.9	20.9	68.0	1.3	-
Cu/ZnO/Al <sub>2</sub> O <sub>3</sub>	85.1	18.8	57.7	6.4	23.2
Al <sub>2</sub> O <sub>3</sub>	266.6	4.2	-	-	-
CuO	10.6	28.1	79.9	-	-

<sup>a</sup> BET surface area was calculated by the BET method.

<sup>b</sup> Average pore diameter from BJH method.

<sup>c</sup> Content of copper was determined by ICP-AES.

<sup>d</sup> Dispersion of copper was calculated with N<sub>2</sub>O-RFC.

<sup>e</sup> Size of copper particles was collected from HAADF images.

**Table S2.** Catalytic performance of Cu-Al catalysts towards MSR reaction.

Catalyst	Methanol	CO	Production rate ( $\mu\text{mol}\cdot\text{g}^{-1}\cdot\text{s}^{-1}$ )			TOF <sup>a</sup> ( $\text{h}^{-1}$ )
	Conversion (%)	Selectivity (%)	CO	CO <sub>2</sub>	H <sub>2</sub>	
2.5Cu/Al <sub>2</sub> O <sub>3</sub>	23.2	0.8	0.11	13.5	44.1	252.2
5Cu/Al <sub>2</sub> O <sub>3</sub>	49.2	0.8	0.22	28.7	93.8	584.9
10Cu/Al <sub>2</sub> O <sub>3</sub>	89.7	0.9	0.46	52.2	147.6	1080.2
15Cu/Al <sub>2</sub> O <sub>3</sub>	49.7	0.9	0.13	14.4	93.6	787.2
Cu/ZnO/Al <sub>2</sub> O <sub>3</sub>	89.0	6.3	3.28	48.9	137.8	1051.2

<sup>a</sup> TOF was evaluated with methanol conversion below 10%. (High WHSV was used to control the methanol conversion. The WHSV was 67.58  $\text{h}^{-1}$  for 2.5Cu/Al<sub>2</sub>O<sub>3</sub>, 124.8  $\text{h}^{-1}$  for 5Cu/Al<sub>2</sub>O<sub>3</sub>, 10Cu/Al<sub>2</sub>O<sub>3</sub> and 5Cu/Al<sub>2</sub>O<sub>3</sub>, 168.96  $\text{h}^{-1}$  for Cu/ZnO/Al<sub>2</sub>O<sub>3</sub>)

**Table S3.** Catalytic performance towards reverse water-gas shift reaction.

Catalyst	CO <sub>2</sub> Conversion (%)	CO production rate ( $\mu\text{mol}\cdot\text{g}^{-1}\cdot\text{s}^{-1}$ )
10Cu/Al <sub>2</sub> O <sub>3</sub>	15.0	2.2
Cu/ZnO/Al <sub>2</sub> O <sub>3</sub>	7.8	1.2

Reaction conditions: 0.1 Mpa, gas flow rate 20  $\text{mL}\cdot\text{min}^{-1}$  for 10%CO<sub>2</sub>/30%H<sub>2</sub>/60%N<sub>2</sub>, 0.1 g catalyst, WHSV = 12000  $\text{mL}\cdot\text{g}^{-1}\cdot\text{h}^{-1}$ .

**Table S4.** Catalytic performance of copper-based catalysts towards MSR reaction.

Samples	T(°C)	X <sub>MeOH</sub> (%)	Acitivity ( $\mu\text{mol}_{\text{H}_2}\cdot\text{g}_{\text{cat}}^{-1}\cdot\text{s}^{-1}$ )	S <sub>CO</sub> (%)
<b>10Cu/Al<sub>2</sub>O<sub>3</sub></b>	<b>250</b>	<b>80.8</b>	<b>147.6</b>	<b>0.9</b>
4.25Cu/Cu(Al)O <sub>x</sub> <sup>[1]</sup>	240	>99	110.8	1
Cu/ZnO <sup>[2]</sup>	250	94.2	105	0.4
Cu/ZnO <sup>[3]</sup>	260	67	99	0.9
Cu/CeO <sub>2</sub> <sup>[3]</sup>	260	91	135	2.3
Cu/CeO <sub>2</sub> <sup>[4]</sup>	270	-	162.9	0.5
Cu/Al <sub>2</sub> O <sub>3</sub> <sup>[3]</sup>	260	22	32	0.4
Cu/ZrO <sub>2</sub> <sup>[5]</sup>	260	100	90	-
Cu-Mn spinel <sup>[6]</sup>	260	92.9	79	0.7
Cu/Cr <sub>2</sub> O <sub>3</sub> <sup>[7]</sup>	240	-	28	5
Cu/CoO <sup>[7]</sup>	240	-	17	14
Cu/Y <sub>2</sub> O <sub>3</sub> <sup>[8]</sup>	300	75	100	-

## References

- [1] H. Meng, Y. Yang, T. Shen, Z. Yin, L. Wang, W. Liu, P. Yin, Z. Ren, L. Zheng, J. Zhang, F.-S. Xiao, M. Wei, Designing Cu<sup>0</sup>-Cu<sup>+</sup> dual sites for improved C-H bond fracture towards methanol steam reforming, *Nat. Commun.*, 14 (2023) 7980.
- [2] T. Shishido, Y. Yamamoto, H. Morioka, K. Takaki, K. Takehira, Active Cu/ZnO and Cu/ZnO/Al<sub>2</sub>O<sub>3</sub> catalysts prepared by homogeneous precipitation method in steam reforming of methanol, *Appl. Catal., A*, 263 (2004) 249-253.
- [3] Y. Liu, T. Hayakawa, T. Tsunoda, K. Suzuki, S. Hamakawa, K. Murata, R.

Shiozaki, T. Ishii, M. Kumagai, Steam reforming of methanol over Cu/CeO<sub>2</sub> catalysts studied in comparison with Cu/ZnO and Cu/Zn(Al)O catalysts, *Top. Catal.*, 22 (2003) 205-213.

[4] Y. Chen, S. Li, S. Lv, Y. Huang, A novel synthetic route for MOF-derived CuO-CeO<sub>2</sub> catalyst with remarkable methanol steam reforming performance, *Catal. Commun.*, 149 (2021) 106215.

[5] C.-Z. Yao, L.-C. Wang, Y.-M. Liu, G.-S. Wu, Y. Cao, W.-L. Dai, H.-Y. He, K.-N. Fan, Effect of preparation method on the hydrogen production from methanol steam reforming over binary Cu/ZrO<sub>2</sub> catalysts, *Appl. Catal., A*, 297 (2006) 151-158.

[6] Q. Liu, L.-C. Wang, M. Chen, Y.-M. Liu, Y. Cao, H.-Y. He, K.-N. Fan, Waste-free Soft Reactive Grinding Synthesis of High-Surface-Area Copper–Manganese Spinel Oxide Catalysts Highly Effective for Methanol Steam Reforming, *Catal. Lett.*, 121 (2008) 144-150.

[7] X. Huang, L. Ma, M.S. Wainwright, The influence of Cr, Zn and Co additives on the performance of skeletal copper catalysts for methanol synthesis and related reactions, *Appl. Catal., A*, 257 (2004) 235-243.

[8] Q. Shen, Z. Cai, Z. Shao, G. Yang, S. Li, Improved performance of bimetallic oxides CuO–Y<sub>2</sub>O<sub>3</sub> synthesized by sol–gel for methanol steam reforming, *J. Am. Chem. Soc.*, 105 (2022) 6839-6850.